

## Supporting Information

### Hydrogen sulfide-generating semiconducting polymer nanoparticles for amplified radiodynamic-ferroptosis therapy of orthotopic glioblastoma

Anni Zhu,<sup>‡a</sup> Shuai Shao,<sup>‡b</sup> Jinyuan Hu,<sup>‡c</sup> Wenzhi Tu,<sup>\*d</sup> Zheming Song,<sup>a</sup> Yue Liu,<sup>a</sup> Jiansheng Liu,<sup>\*e</sup>

Qin Zhang,<sup>\*f</sup> and Jingchao Li<sup>\*a</sup>

<sup>a</sup> *State Key Laboratory for Modification of Chemical Fibers and Polymer Materials, College of Biological Science and Medical Engineering, Donghua University, Shanghai 201620, China. E-mail: jcli@dhu.edu.cn*

<sup>b</sup> *Department of Burns and Plastic Surgery, Nanjing Drum Tower Hospital, The Affiliated Hospital of Nanjing University Medical School, Nanjing 210008, China.*

<sup>c</sup> *Faculty of Arts and Sciences, Key Laboratory of Cell Proliferation and Regulation Biology of Ministry of Education, Center for Biological Science and Technology, Guangdong Zhuhai-Macao Joint Biotech Laboratory, Beijing Normal University, Zhuhai 519087, China.*

<sup>d</sup> *Department of Radiation Oncology, Shanghai General Hospital, Shanghai Jiao Tong University School of Medicine, Shanghai 201620, China. E-mail: wenzhitu@126.com*

<sup>e</sup> *Department of Neurology, Shanghai Xuhui District Central Hospital, Zhongshan-Xuhui Hospital Fudan University, Shanghai 200032, China. E-mail: drjianshengliu84@gmail.com*

<sup>f</sup> *Institute of Translational Medicine, Shanghai University, Shanghai 200444, China. E-mail: Sabrina\_1985@shu.edu.cn*

<sup>‡</sup> *These authors contributed equally to this work.*

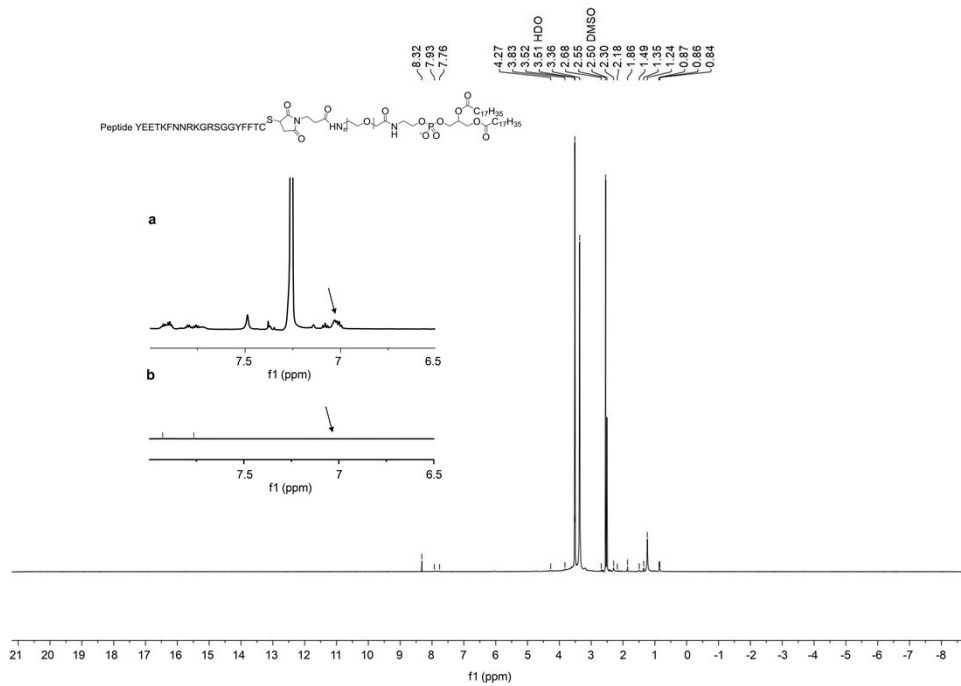


**Fig. S1.**  $^1\text{H}$  NMR spectrum of DSPE-PEG-Ang in  $\text{DMSO-d}_6$ .

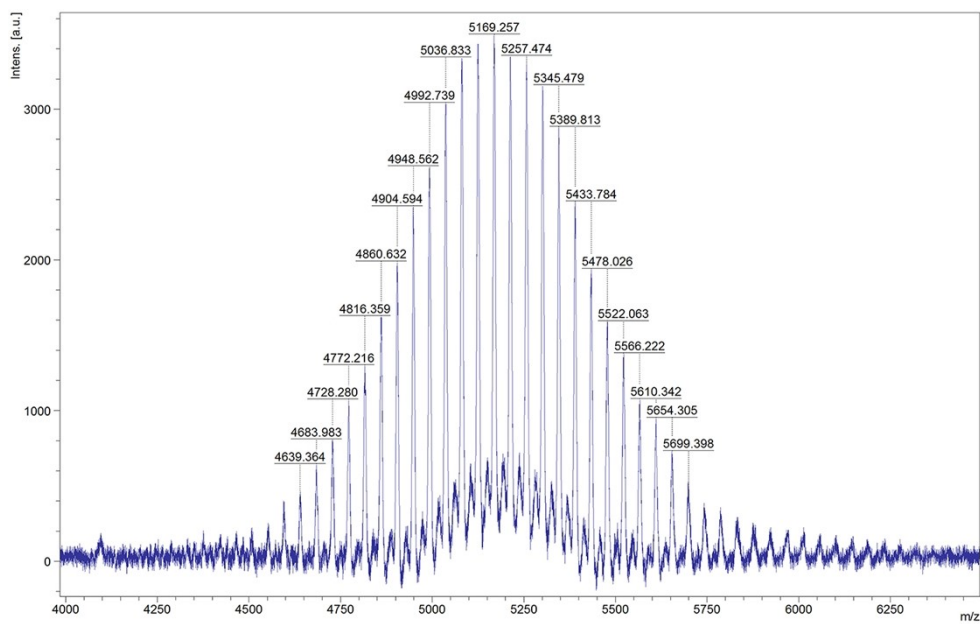


**Fig. S2.** Analysis of molecular weight of DSPE-PEG-Ang confirmed by MALDI-TOF-MS.

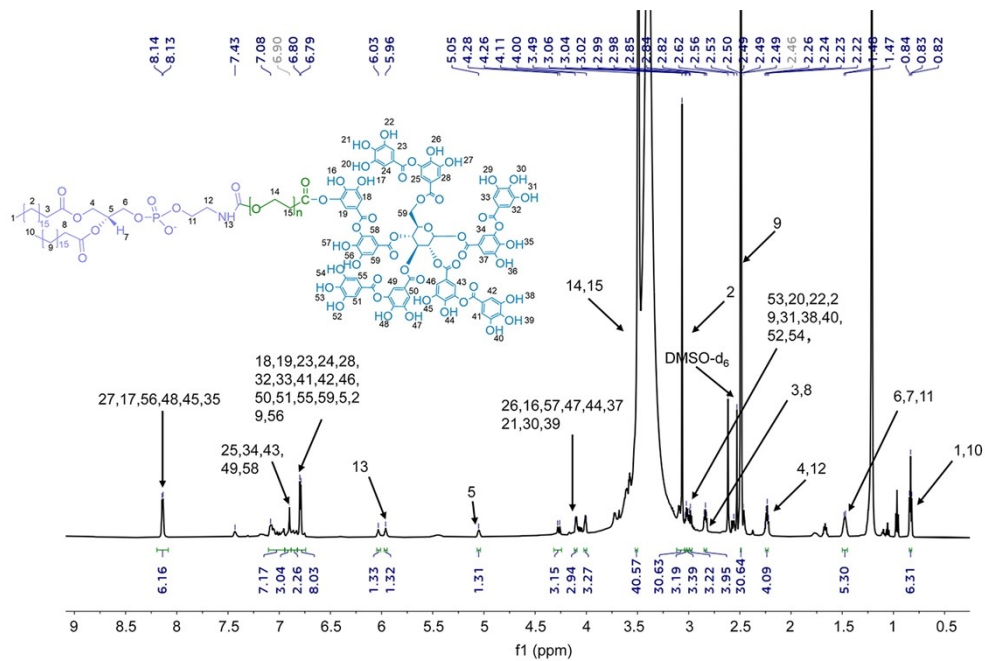


**Fig. S3.**  $^1\text{H}$  NMR spectrum of DSPE-PEG-TA in  $\text{DMSO-d}_6$ .

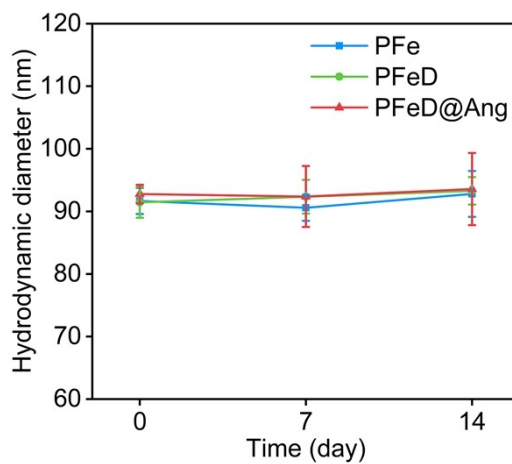


**Fig. S4.** Hydrodynamic diameters of PFe, PFeD and PFeD@Ang in water on different days ( $n = 3$ ).

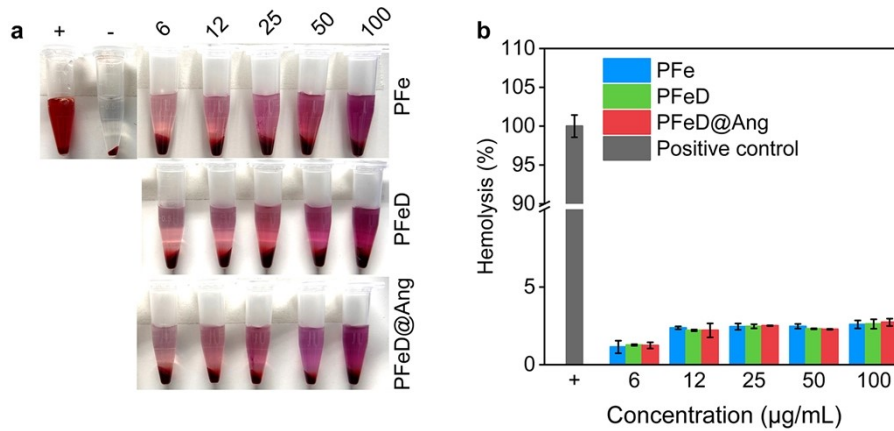


**Fig. S5.** (a) Photographs of erythrocytes after co-incubation with PBS (-), water (+), PFe, PFeD and PFeD@Ang at different concentrations. (b) Hemolysis rates of erythrocytes after co-incubation with water (+), PFe, PFeD and PFeD@Ang (n = 3).

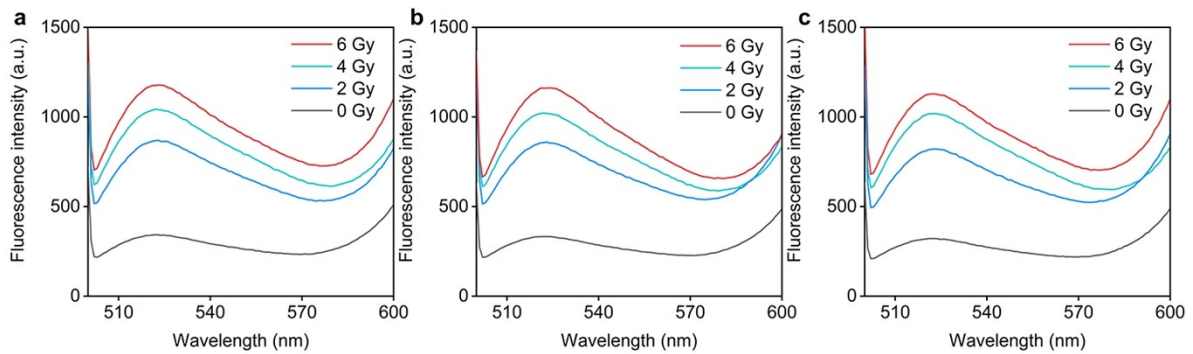


**Fig. S6.** Fluorescence spectra of SOSG in solutions containing PFe, PFeD and PFeD@Ang with or without X-ray irradiation.

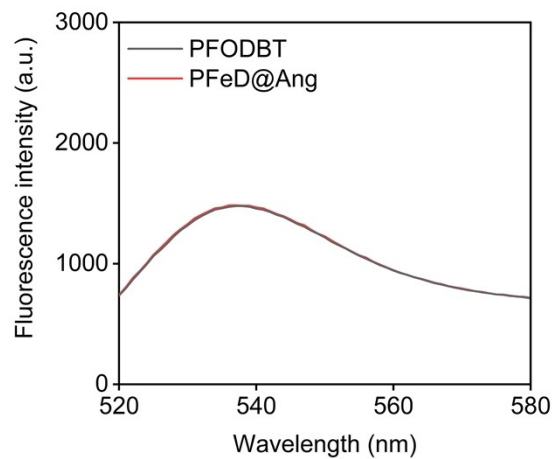


**Fig. S7.** Fluorescence spectra of SOSG in solutions containing PFODBT and PFeD@Ang with X-ray irradiation (PFODBT concentration = 25  $\mu\text{g}/\text{mL}$ , 4Gy).

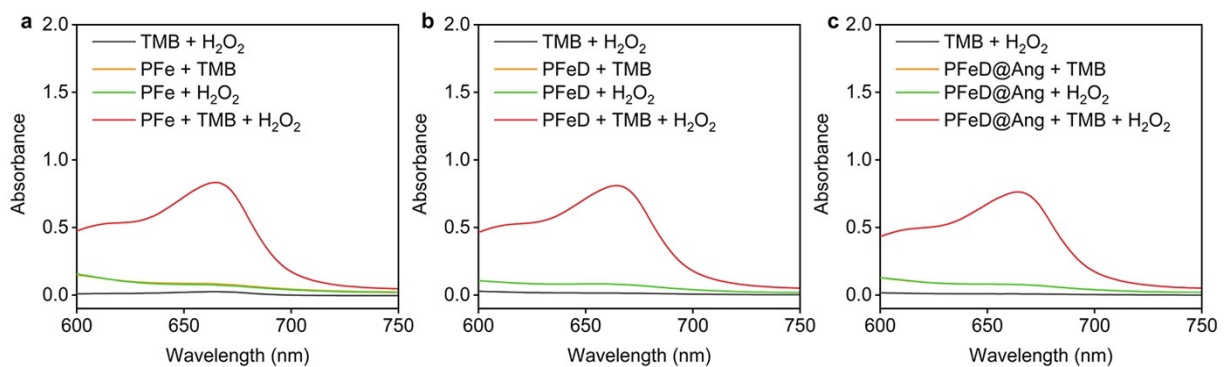


**Fig. S8.** The  $\cdot\text{OH}$  generation evaluation using TMB as the probe for (a) PFe, (b) PFeD and (c) PFeD@Ang in the presence of  $\text{H}_2\text{O}_2$  (100  $\mu\text{M}$ ).

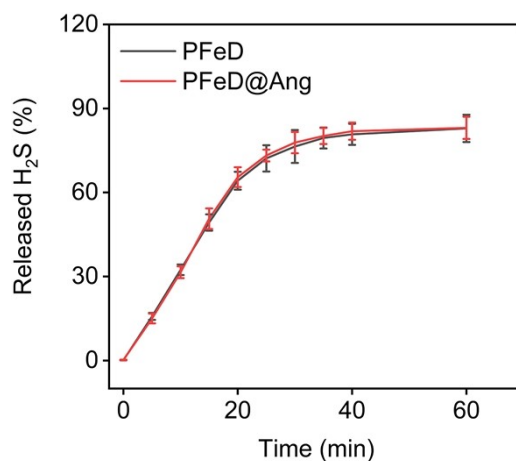


**Fig. S9.** Release percentages of  $\text{H}_2\text{S}$  donor from PFeD and PFeD@Ang at pH 5.5 over time (n = 3).

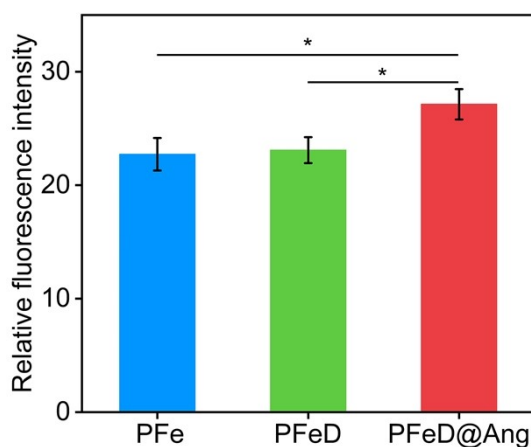


**Fig. S10.** Fluorescence intensity of GL261-luc cancer cells after incubation with PFe, PFeD and PFeD@Ang (n = 3).

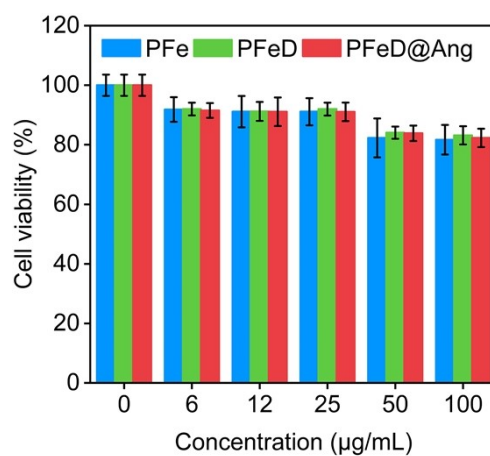


**Fig. S11.** Cell viability of GL261-luc cancer cells after incubation with PFe, PFeD and PFeD@Ang at different concentrations for 24 h (n = 3).

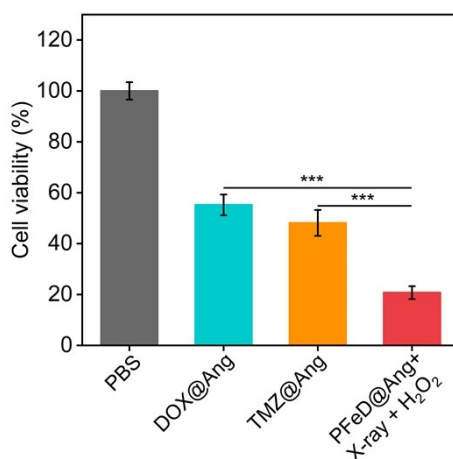


**Fig. S12.** Viability of GL261-luc cancer cells after different treatments (n = 3).

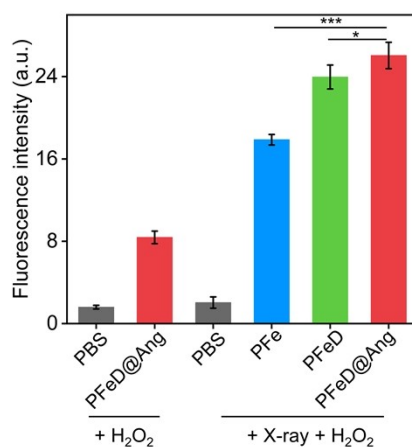


**Fig. S13.** Quantitative fluorescence intensity of H<sub>2</sub>DCFDA-treated GL261-luc cancer cells after various treatments (n = 3).

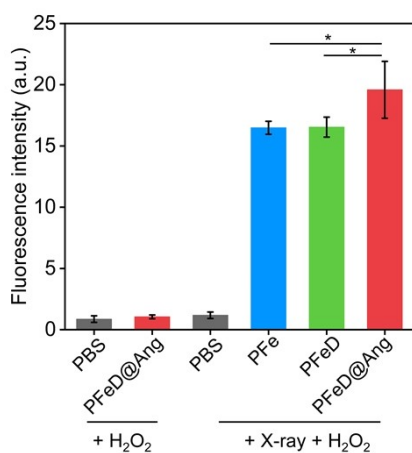


**Fig. S14.** Quantitative fluorescence intensity of  $\gamma$ -H2AX-treated GL261-luc cancer cells after different treatments (n = 3).

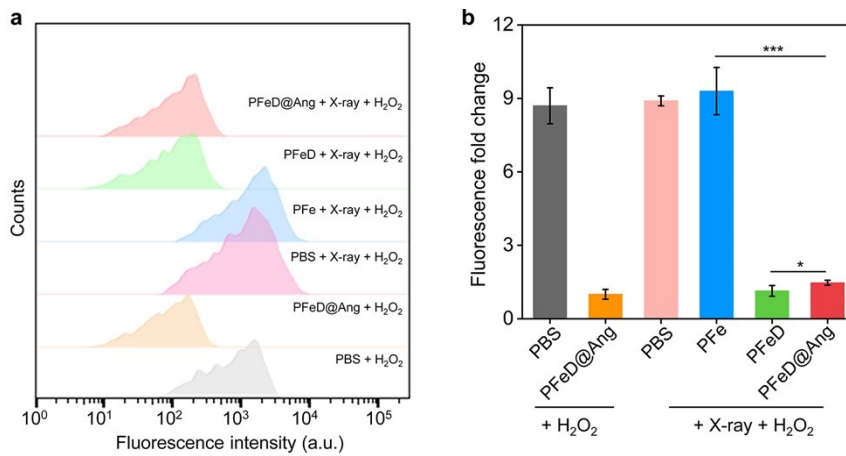


**Fig. S15.** (a) Fluorescence intensity analysis of oxygen indicator in orthotopic glioma tumors of each group. (b) Fluorescence intensity changes of oxygen indicator in orthotopic glioma tumors of each group (n = 3).

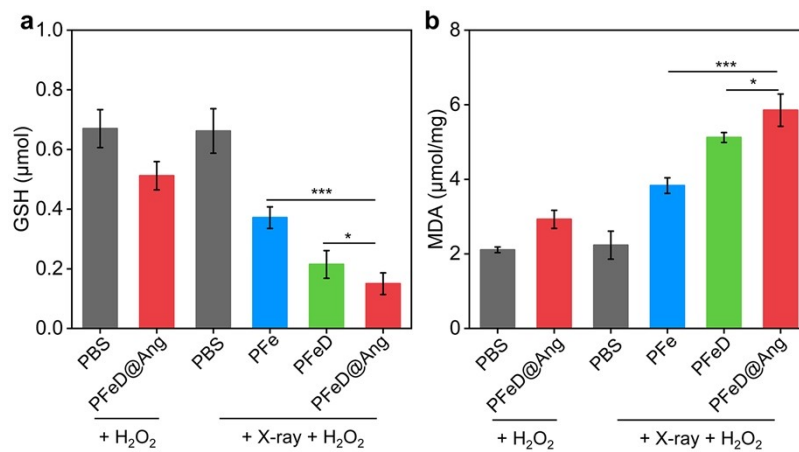


**Fig. S16.** (a) In vitro assessment of GSH levels in GL261-luc cancer cells (n = 5). (b) Evaluation of MDA levels in GL261-luc cancer cells (n = 5).

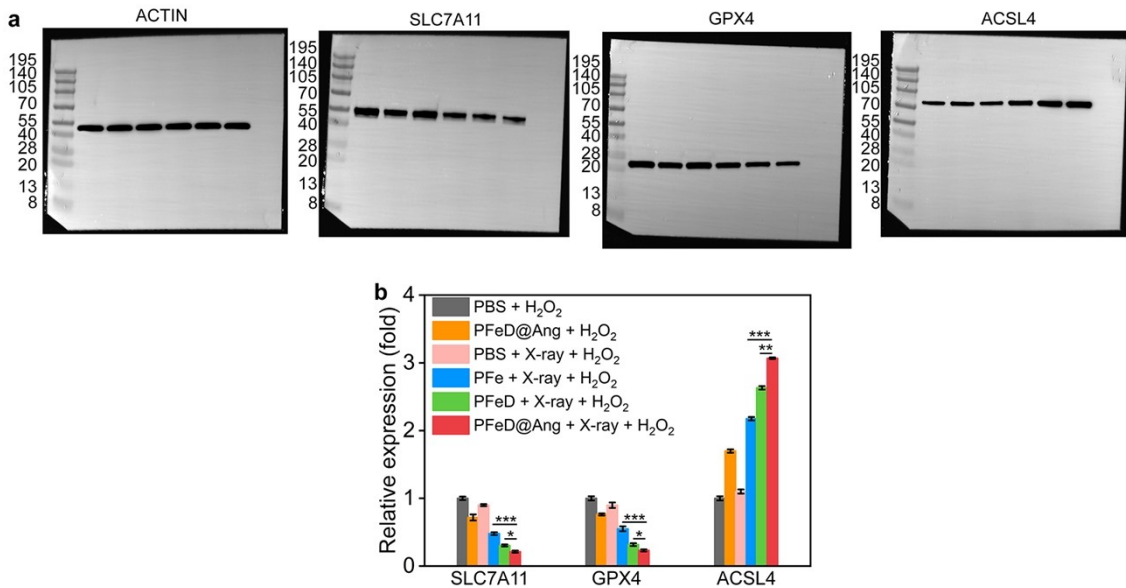


**Fig. S17.** (a) Uncropped original images of WB in Fig. 4e. (b) Quantification of SLC7A11, GPX4, and ACSL4 protein levels in GL261-luc cancer cells (n = 3).

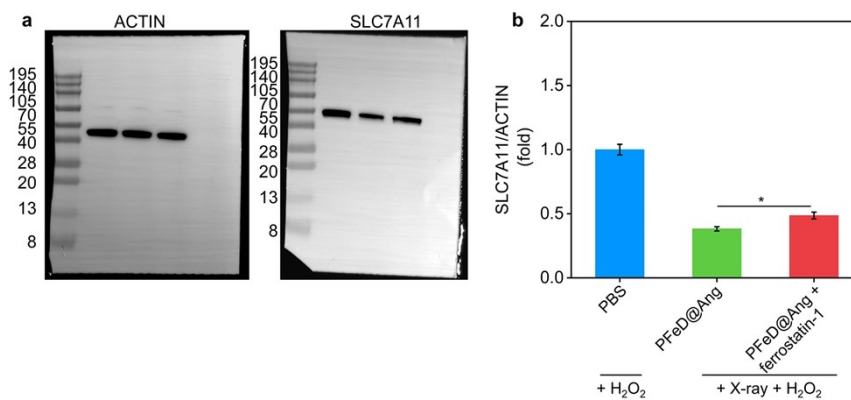


**Fig. S18.** (a) Uncropped original images of WB in Fig. 4g. (b) Quantification of SLC7A11 protein levels in GL261-luc cancer cells (n = 3).

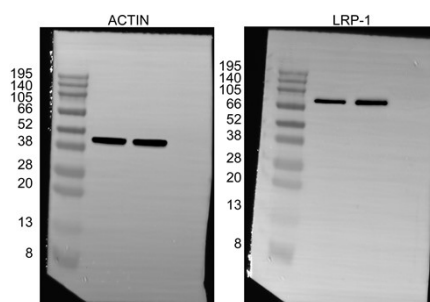


**Fig. S19.** Uncropped original images of WB in Fig. 5b.



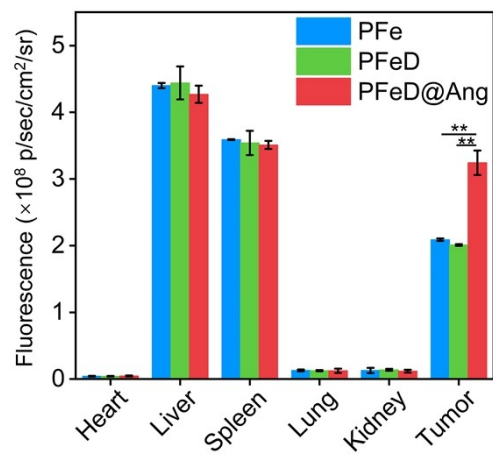


**Fig. S20.** Analysis of fluorescence intensity of different tissues (n = 5).

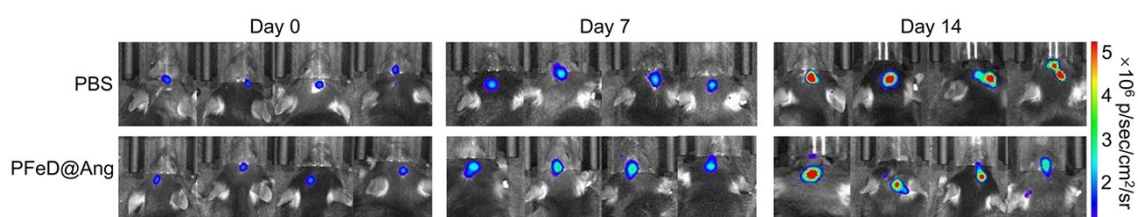


**Fig. S21.** Representative bioluminescence (BL) pictures of mice with orthotopic GL261-luc glioma on day 0, 7 and 14 following PBS and PFeD@Ang treatments (n = 4).

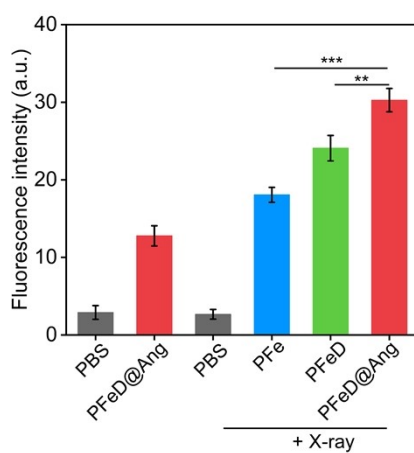


**Fig. S22.** Fluorescence intensity of the generated ROS signals in tumors for PBS-, PFe-, PFeD- and PFeD@Ang-injected mice without or with X-ray irradiation (n = 5).

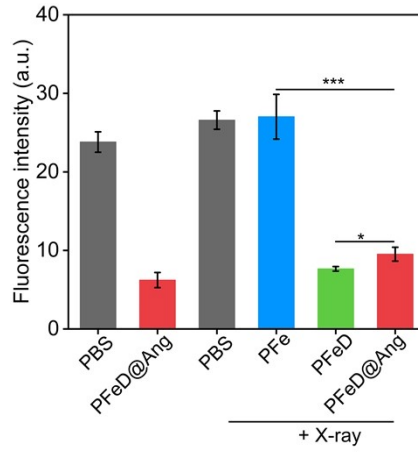


**Fig. S23.** Fluorescence intensity of HIF-1 $\alpha$  signals in tumors for PBS-, PFe-, PFeD- and PFeD@Ang-injected mice without or with X-ray irradiation (n = 5).

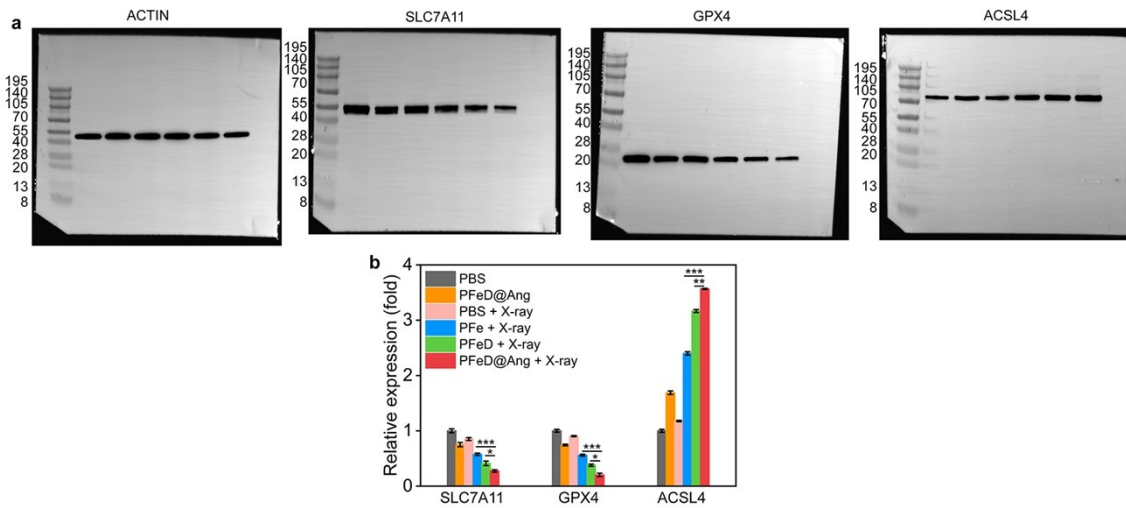


**Fig. S24.** (a) Uncropped original images of WB in Fig. 7e. (b) Quantification of SLC7A11, GPX4, and ACSL4 protein levels in tumor (n = 3).

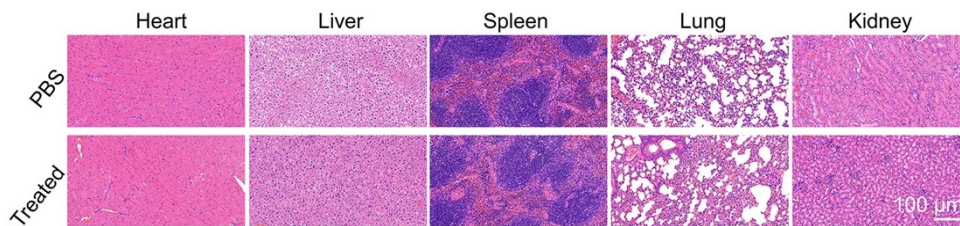


**Fig. S25.** Histological H&E staining images of heart, liver, spleen, lung and kidney in PBS and treated (PFeD@Ang + X-ray) groups after different treatments for 14 days.

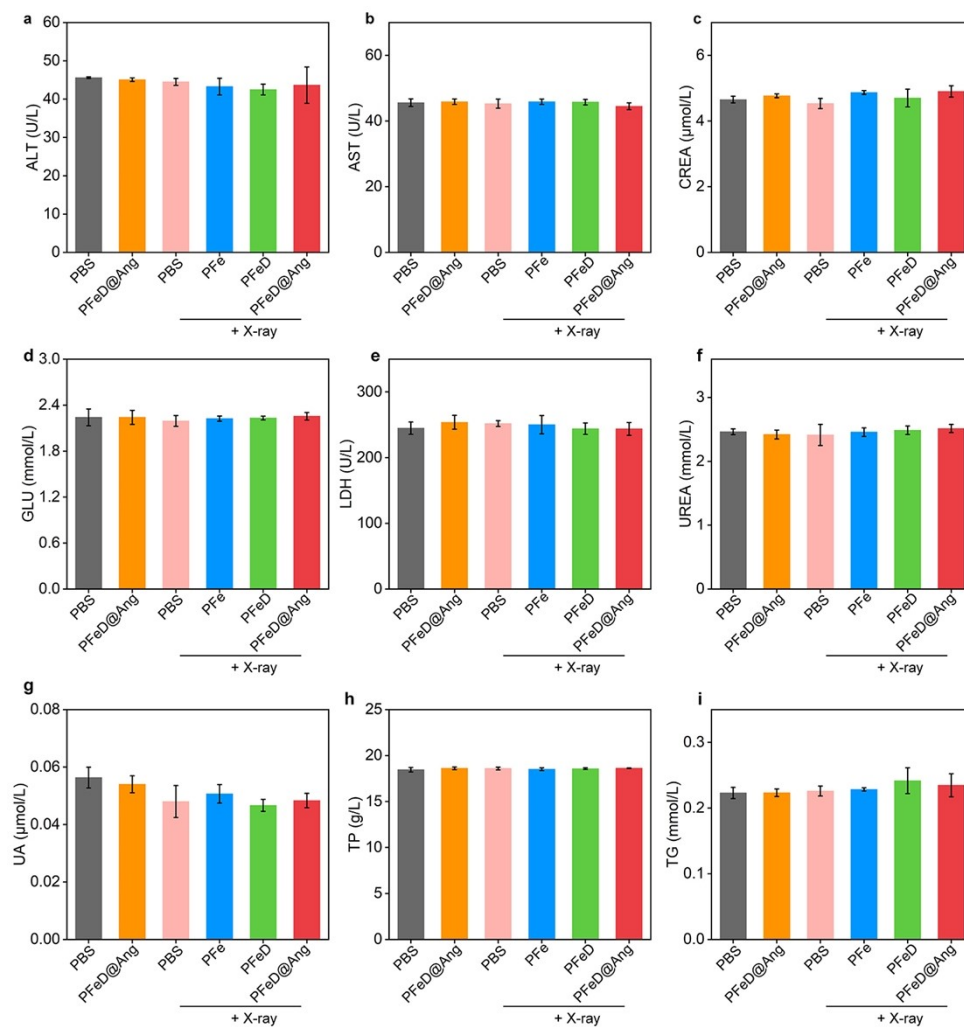


**Fig. S26.** Blood biochemistry analysis of (a) alanine aminotransferase (ALT), (b) aspartate aminotransferase (AST), (c) creatinine (CREA), (d) glucose (GLU), (e) lactate dehydrogenase (LDH), (f) UREA, (g) uric acid (UA), (h) total protein (TP) and (i) triglyceride (TG) in living mice after various treatments (n = 5).

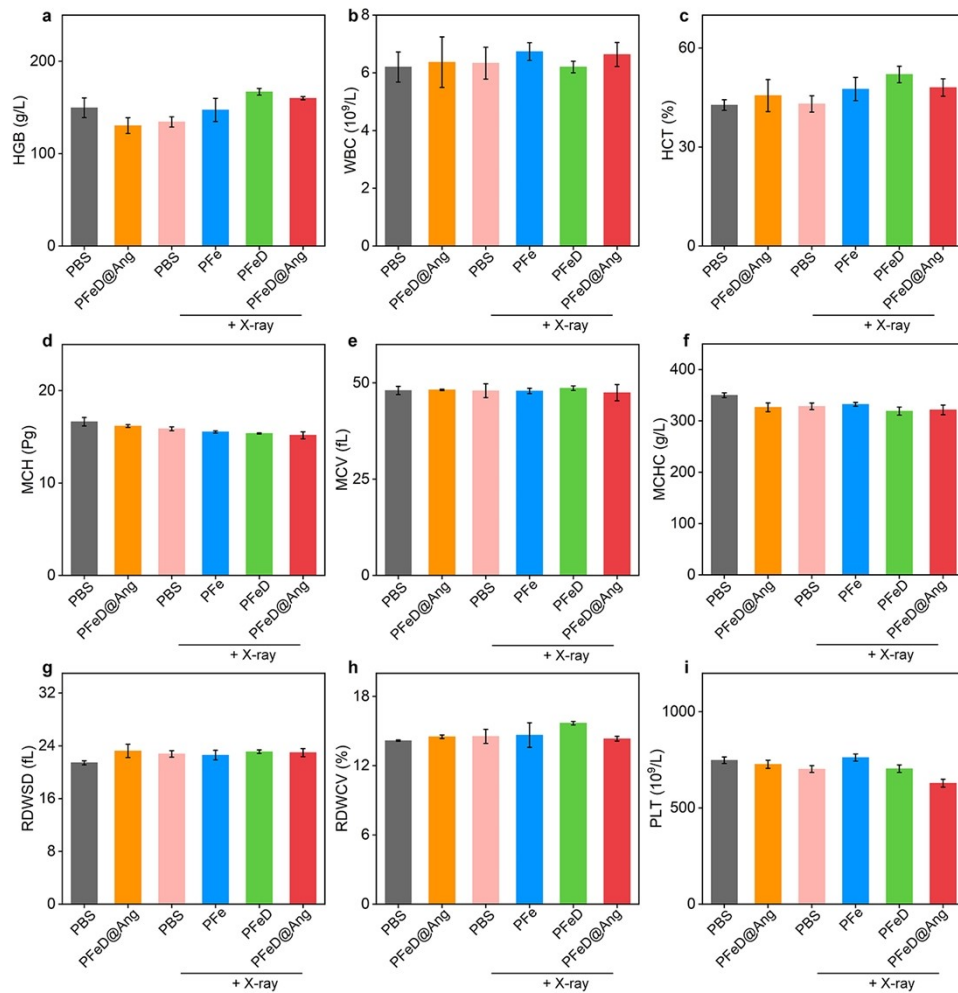


**Fig. S27.** Blood routine analysis of (a) hemoglobin (HGB), (b) white blood cell (WBC), (c) Hematocrit (HCT), (d) mean corpuscular hemoglobin (MCH), (e) mean corpuscular volume (MCV), (f) mean corpuscular hemoglobin concentration (MCHC), (g) red blood cell distribution width standard deviation (RDWSD), (h) red blood cell distribution width coefficient of variation (RDWCV) and (i) platelet (PLT) in living mice after various treatments (n = 5).

## Experimental section

### Characterization technique

UV-visible absorbance and fluorescence spectra of PFe, PFeD, and PFeD@Ang were obtained using a Persee spectrophotometer (TU-1810) and a SHIMADZU spectrophotometer (RF-6000, Japan). Hydrodynamic diameters and zeta potentials were measured with a Malvern Zetasizer (NanoZS90). Transmission electron microscopy (TEM, Tecnai G2) characterized the morphology. Nuclear magnetic resonance ( $^1\text{H}$  NMR) spectra of DSPE-PEG-TA and DSPE-PEG-Ang were obtained using a Bruker NMR spectrometer (400 MHz). MALDI-TOF-MS was employed to measure the molecular weight of DSPE-PEG-Ang (Bruker autboflex speed, Germany). The irradiation was carried out using an X-ray equipment known as the MultiRad 225 (Tucson, Arizona, USA).

### Synthesis of DSPE-PEG-Ang

To synthesize DSPE-PEG-Ang, DSPE-PEG-Mal (20 mg) and angiopep-2 (20 mg) were dissolved in PBS solution (DSPE-PEG-Mal/angiopep-2 = 2:1, mol/mol) and react at 4 °C for 12 hours. Through freeze-drying and dialysis, the product was purified.

### Synthesis of DSPE-PEG-TA-Fe

According to our previous work,<sup>1</sup> DSPE-PEG-COOH (100 mg, 45  $\mu\text{M}$ ), EDC (18 mg, 90  $\mu\text{M}$ ), and DMAP (6 mg, 45  $\mu\text{M}$ ) were dissolved in 2 mL of dichloromethane and stirred at room temperature for 24 hours. At room temperature, TA (13 mg, 45  $\mu\text{M}$ ) solution was slowly added, and the mixture was stirred for another 24 hours. A vacuum was applied to evaporate organic solvents, followed by dialysis and freeze-drying of the product to obtain DSPE-PEG-TA. DSPE-PEG-TA was then stirred at room temperature for 24 hours with  $\text{FeCl}_3$  solution (10 mM) to yield DSPE-PEG-TA-Fe.

### Synthesis of PFe, PFeD and PFeD@Ang

Tetrahydrofuran (THF) was used to dissolve PFODBT (0.5 mg),  $\text{H}_2\text{S}$  donor (0.5 mg), and DSPE-PEG-Ang (10.0 mg). The resulting solution was then injected into a THF and water mixing solution ( $V_{\text{THF}}:V_{\text{water}} = 1:9$ ). THF was eliminated by evaporation following a 5-minute sonication, and the resultant product was subsequently ultrafiltered to obtain PFeD@Ang. Using THF we dissolved PFODBT (0.5 mg),  $\text{H}_2\text{S}$  donor (0.5 mg), and DSPE-mPEG (10.0 mg). After that, the resultant solution ( $V_{\text{THF}}:V_{\text{water}} = 1:9$ ) was injected into a THF and water mixing solution. After a 5-minute sonication,

THF was removed by evaporation. The resulting product was then ultrafiltered to yield PFeD. The compounds PFODBT (0.5 mg), DSPE-mPEG (10.0 mg), and DSPE-PEG-TA-Fe (10.0 mg) were dissolved using THF. After that, the resultant solution ( $V_{\text{THF}}:V_{\text{water}} = 1:9$ ) was injected into a THF and water mixing solution. After 5 minutes of sonication, PFe was obtained by evaporation and ultrafiltration.

### **Synthesis of DOX@Ang and TMZ@Ang**

Tetrahydrofuran (THF) was used to dissolve DOX (0.5 mg), DSPE-mPEG (10 mg), and DSPE-PEG-Ang (10.0 mg). The resulting solution was injected into a THF/water mixture ( $V_{\text{THF}}:V_{\text{water}} = 1:9$ ). After 5 minutes of sonication, THF was evaporated, and the product was ultrafiltered to obtain DOX@Ang. Similarly, TMZ (0.5 mg), DSPE-mPEG (10 mg), and DSPE-PEG-Ang (10.0 mg) were dissolved in THF, and the solution ( $V_{\text{THF}}:V_{\text{water}} = 1:9$ ) was injected into a THF/water mixture. Following 5 minutes of sonication, THF was removed by evaporation, and the product was ultrafiltered to yield TMZ@Ang.

### **In vitro cytotoxicity and therapeutic effect assays**

The cytotoxicity of PFe, PFeD, and PFeD@Ang was assessed using a CCK-8 assay after 24 hours of co-incubation. To evaluate the in vitro therapeutic efficacy, GL261-luc cells were cultured with PBS, DOX@Ang, TMZ@Ang, PFe, PFeD, or PFeD@Ang (PFODBT concentration = 25  $\mu\text{g}/\text{mL}$ ) for 12 hours, followed by 4 Gy X-ray irradiation and subsequent CCK-8 measurements

### **DNA damage evaluation**

GL261-luc cells were cultured with PFe, PFeD, and PFeD@Ang (PFODBT concentration = 25  $\mu\text{g}/\text{mL}$ ) for 12 hours, followed by exposure to 4 Gy X-ray irradiation. Cells were stained with Alexa Fluor 488-labeled goat anti-rabbit IgG (H+L) for 1 hour and DAPI for 30 minutes, then washed with PBS. Fluorescence signals were observed by confocal laser scanning microscopy (CLSM, Carl Zeiss LSM 700) to assess DNA damage.

### **In vitro evaluation of MDA and GSH levels**

GL261-luc cells were incubated with PBS, PFe, PFeD, and PFeD@Ang (25  $\mu\text{g}/\text{mL}$  PFODBT), then exposed to 4 Gy X-ray. After treatment, cells were collected, washed with PBS, and intracellular MDA and GSH levels measured using assay kits.

### **Ferroptosis-related protein expression in vitro**

Following different treatments, GL261-luc cells were collected for protein extraction and then rinsed with PBS. The levels of intracellular expression of ACSL4, GPX4 and SLC7A11 were then measured by WB. Total proteins were extracted from cells using lysis buffer containing phosphorylation inhibitors and protease inhibitors. After separation by SDS-PAGE, the proteins were transferred to a PVDF membrane. The membrane was incubated for 1 hour with blocking buffer (TBST containing 5% nonfat dry milk), followed by overnight incubation with the primary antibody at 4°C. The next day, the membrane was incubated with the secondary antibody at room temperature for 2 hours. Finally, the membrane was exposed to a chemiluminescent substrate (Thermo Fisher Scientific, USA). Antibodies for ACSL4, GPX4 and SLC7A11 were purchased from Abcam.

### ***In vitro* evaluation of BBB penetrating efficacy**

The *in vitro* BBB model was established based on our previous work.<sup>2</sup> In brief, bEnd.3 cells were plated in the upper chambers of six-well transwell plates and cultured for 7 days with periodic medium changes. The successful formation of the BBB model was verified when the transendothelial electrical resistance exceeded 200  $\Omega$  cm<sup>2</sup> (RE1600). The fluorescence intensity of nanoparticles in the upper and lower chambers was measured to determine the permeability, and fluorescence images were acquired by laser scanning confocal microscopy.

### **References**

1. L. Zhu, X. Wang, M. Ding, N. Yu, Y. Zhang, H. Wu, Q. Zhang, J. Liu and J. Li, *Biomater. Sci.*, 2023, **11**, 6823-6833.
2. M. Ding, A. Zhu, Y. Zhang, J. Liu, L. Lin, X. Wang and J. Li, *Nano Today*, 2024, **57**, 102398.